Hindawi
Wireless Communications and Mobile Computing
Volume 2021, Article ID 5589487, 10 pages
https://doi.org/10.1155/2021/5589487

Research Article

Empirical Path Loss Channel Characterization Based on Air-to-Air Ground Reflection Channel Modeling for UAV-Enabled Wireless Communications

Jatuporn Supramongkonset,[1] Sarun Duangsuwan,[2] Myo Myint Maw,[3] and Sathaporn Promwong[1]

[1]*Electrical Engineering, Faculty of Engineering, King Mongkut's Institute of Technology Ladkrabang (KMITL), Bangkok 10520, Thailand*
[2]*Innovative Wireless and IoT Laboratory (IWIoT), Electrical Engineering, Department of Engineering, Prince of Chumphon Campus, King Mongkut's Institute of Technology Ladkrabang (KMITL), Pathio, Chumphon 86160, Thailand*
[3]*Department of Computer Engineering and Information Technology, Mandalay Technological University (MTU), Patheingyi Township, Mandalay, Myanmar*

Correspondence should be addressed to Sarun Duangsuwan; ax_sarun@hotmail.com

Received 24 February 2021; Revised 4 June 2021; Accepted 12 July 2021; Published 2 August 2021

Academic Editor: Rehmat Ullah

The purpose of this work was to investigate the air-to-air channel model (A2A-CM) for unmanned aerial vehicle- (UAV-) enabled wireless communications. Specifically, a low-altitude small UAV needs to characterize the propagation mechanisms from ground reflection. In this paper, the empirical path loss channel characterizations of A2A ground reflection CM based on different scenarios were presented by comparing the wireless communication modules for UAVs. Two types of wireless communication modules both WiFi 2.4 GHz and LoRa 868 MHz frequency were deployed to study the path loss channel characterization between Tx-UAV and Rx-UAV. To investigate the path loss, three types of experimental channel models, such as CM1 grass floor, CM2 soil floor, and CM3 rubber floor, were considered under the ground reflection condition. The analytical A2A Two-Ray (A2AT-R) model and the modified Log-Distance model were simulated to compare the correlation with the measurement data. The measurement results in the CM3 rubber floor scenario showed the impact from the ground reflection at 1 m to 3 m Rx-UAV altitudes both 2.4 GHz and 868 MHz which was converged to the A2AT-R model and related to the modified Log-Distance model above 3 m. It clear that there is no ground reflection effect from the CM1 grass floor and CM2 soil floor. This work showed that the analytical A2AT-R model and the modified Log-Distance model can deploy to model the path loss of A2A-CM by using WiFi and LoRa wireless modules.

1. Introduction

The numerous deployments of Internet of Things (IoT) devices such as IoT-based WiFi IEEE 802.11 [1], LoRa-based low power wide area network (LPWAN) [2], Narrow-band IoT (NB-IoT) [3], or Sigfox [4] that uses in modern applications such as healthcare [5], transportation [6], smart farming [7], smart cities [8], and among others [9]. The fundamental challenges of IoT communications are channel modeling, connectivity, coverage, reliability, latency, and energy efficiency. Especially, the propagation limitation of IoT devices significantly impacts the coverage range and reliability of communication systems. Therefore, it is necessary to have an analytic channel modeling that can resolve the IoT requirements for deep coverage, reliability, and energy efficiency.

Likewise, the air-to-ground (A2G) channel modeling is one of the challenges in the UAV-enabled wireless communication [10]. While the A2A channel modeling is newly challenging for vehicle-to-vehicle (V2V) networking [11]. Then,

the channel modeling of UAV significantly requires for IoT and 5G applications [12]. For IoT group devices, frying UAVs likes the mobile Base Station (BS). The UAV-enabled BS can effectively support IoT services in both uplink and downlink scenarios across scattered geographical areas. For the uplink, the UAV can dynamically move based on IoT locations to collect the data in energy efficiency and reliability. The applied work of UAV-enabled BS was presented in [13]. For the downlink, the UAV BS can be optimally deployed close to IoT devices and increased the coverage area for IoT systems [14]. Clearly that, the use of UAVs and IoT significantly requires the connectivity of wireless communication modules such as WiFi or LoRa modules.

The LoRa communication is clustered in LPWAN groups as well as Sigfox and NB-IoT. Using the LoRa communication for UAVs is mostly discussed about the energy efficiency of long-distance [15, 16]. Specifically, the performance requirement for communications between multiple UAVs and ground stations has been specified by swarm UAVs, 3GPP TS 22.261, TR 22.261, and TR 36.777 [17]. To deploy the swarm UAVs, the A2A-CM needs to analyze in different environments. Due to the large-scale propagation, the A2A-CM are suffered from free space path loss, ground reflection, dropper, and shadowing. Compared with the mobile wireless channel, the UAV-based A2G channel and A2A channel will often be more dispersive, incur larger terrestrial shadowing attenuation, and change more rapidly. By using the LoRa module, the UAV communication channel was presented in [18]. The use of the LoRa module can stable the performance of signal strength and high precision in long-distance. Due to the Chirp Spread Spectrum (CSS) modulation, the communication link in the air of the LoRa module is more efficient [19]. In addition, the channel model of LoRa at 433 MHz and 868 MHz was presented in [20] based on ground-to-ground (G2G) CM; the authors investigated the path loss-based empirical measurement in the urban environment. Aforementioned, the use of LoRa is beneficial for smart city applications such as air pollution monitoring on UAV [21] or smart agricultural application such as soil quality analysis [22] and so on.

Regarding the potential of path loss modeling, several works have been focused on optimally predicted path loss, channel prediction. In [23], the authors presented A2A path loss prediction based on machine learning. The simulation model by using the ray-tracing method has been utilized to formulate the data for the A2A channel. They assumed that the Tx-UAV was equipped with a directional antenna and Rx-UAV moved at a spacing of 2 m with different of both Tx-UAV and Rx-UAV altitudes. Then, the path loss results were predicted by using kNN and random forest algorithms. Although the results were satisfied by using a random forest algorithm, there is no consideration under the realistic environments of UAV communication channels. Then, the path loss prediction model under the realistic environments was presented by using kNN and random forest algorithm for A2G-CM [24]. The results indicate that the random forest algorithm outperformed the kNN for channel prediction. The related works of path loss prediction modeling by using machine learning algorithms were studied in [25, 26]. Aforementioned in path loss prediction of A2A-CM and A2G-CM, using machine learning can optimally predict the uncertainty of path loss characteristics.

For A2A-CM, the comprehensive survey on UAV channel modeling was described in [27] where the propagation channel of the high-altitude UAV A2A links depends on the free space model and dropper shift, while the low-altitude needs to consider the ground reflection and shadowing. In general, the target of A2A communication is applying UAVs as a relay networking for multihop communications. In [28], the authors presented the A2A data link capable of supporting addressed, multicast, and broadcast for multihop communications. They proposed suitable methods such as a medium access scheme, forward error correction codes, and modulation scheme for the A2A data link. Meanwhile, the propagation characteristics for the A2A channel were investigated in urban environments [29]. The authors described the ray-tracing technique that can use to formulate the path loss in a large-scale fading channel. It shows that the excess fading loss (EL) and close-in free space (CI) can apply as a simple tool for the A2A channel model. Afterward, the path loss of the A2A channel for the flying ad hoc network (FANET) was examined by using the SUI model [30]. The simulation data considered path loss for flying over rugged terrains. It can be seen that the results were uncorrelated with the propagation environments. Indeed, the SUI model may be unsuitable for the A2A channel model. Likewise, the wideband A2A channel model has been simulated as a model for the suitability of drone-to-drone communications [31]. The simulation results were accordant to the realistic propagation mechanisms where the results reveal rich multipath from the ground reflection. To describe the ground reflection, the angle-of-arrival (AOA) and angle-of-departure (AOD) for ground scattering were presented for A2A channel modeling [32]. The authors proposed some methodologies that can conveniently analyze multiscattering cluster scenarios such as the Three-dimensional (3D) wideband nonstationary has been described for A2A-CM in [33, 34]. However, the consideration of the ground reflection condition under the realistic environments for drone-to-drone communications or small UAVs is lacking.

In this paper, an empirical path loss channel characterization of A2A-CM under the ground reflection model is presented. Indeed, the path loss characteristic for the low-altitude A2A-CM depends on free space loss, shadowing, and the two-ray model. Thus, we consider the path loss two-ray model by using the analytical A2AT-R model and the modified Log-Distance model. The measurement is investigated under the ground reflection scenario cases such as CM1 grass floor, CM2 soil floor, and CM3 rubber floor, respectively. The reasons for the consideration in grass floor, soil floor, and rubber floor are the scenarios for smart farming and stadium. Using both WiFi-based 2.4 GHz and LoRa-based 868 MHz, the Tx-UAV and Rx-UAV are applied because both the wireless modules are small IoTs that can be equipped on the small UAV. The experimental results show the path loss measured data, the analytical A2AT-R model, and the modified Log-Distance model for CM1, CM2, and CM3, respectively. To verify the measurement scenarios, we

assume that these CM scenarios are set up as the case study of ground reflection models of small UAV-enabled wireless communications.

The remainder of this paper is organized as follows. The analysis of path loss models describes in Section 2. In Section 3, the measurement setups in the different scenarios are presented. Section 4 describes the results and discussion for the ground reflection model in UAV-enabled wireless communications. Finally, the conclusion is given in Section 5.

2. Analysis of Path Loss Models

2.1. Analytical A2AT-R Model. The geometric of the A2AT-R model is shown in Figure 1. The total received E-field at the Rx-UAV is $E_U(d_c)$, given that the direct line-of-sight (LOS) component, $E(d')$, and the ground reflected component, $E_r(d'')$

$$E_U(d_c) = E\left(d'\right) + E_r\left(d''\right). \tag{1}$$

Two propagation waves arrive at the Rx-UAV: the direct wave that travels distance d' and the reflected wave that travels distance d''. Thus, d_c is the separation distance between Tx-UAV and Rx-UAV. The E-field due to the LOS at the Rx-UAV can be expressed as

$$E\left(d'\right) = \frac{E_0 d_0}{d'} \cos\left(2\pi f_c\left(t - \frac{d'}{c}\right)\right), \tag{2}$$

and the E-field for the ground reflected wave, which has a propagation distance of d'', can be expressed as

$$E_r\left(d''\right) = \Gamma_{Floor} \frac{E_0 d_0}{d''} \cos\left(2\pi f_c\left(t - \frac{d''}{c}\right)\right), \tag{3}$$

where f_c is the carrier frequency, c is the velocity of the light, and E_0 is the free space E-field at a reference distance d_0 from the Rx-UAV, then $d > d_0$. Γ_{Floor} denotes the reflection coefficient from the floors.

The $E_U(d_c)$ can be rewritten as

$$\begin{aligned} E_U(d_c) = {} & \frac{E_0 d_0}{d'} \cos\left(2\pi f_c\left(t - \frac{d'}{c}\right)\right) \\ & + (-1)\frac{E_0 d_0}{d''} \cos\left(2\pi f_c\left(t - \frac{d''}{c}\right)\right), \end{aligned} \tag{4}$$

where $\Gamma_{\text{Floor}} = -1$ denotes the perfect ground reflection component from the floor.

In term of received signal strength indicator (RSSI), we obtain the received signal for the analytical A2AT-R model, that $r_{T-R}(t)$ can be written as

$$r_{T-R}(t) = \left(\frac{\lambda}{4\pi}\left|r_{d'}(t) + r_{d''}(t)\right| \cdot e^{j2\pi f_c t}\right), \tag{5}$$

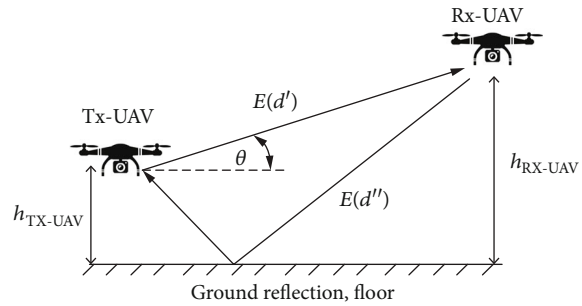

Figure 1: The geometric of analytical A2AT-R model.

where

$$\begin{aligned} r_{d'}(t) &= \frac{\sqrt{G_{T,d'} G_{R,d'}}}{d_0} e^{-j2\pi\frac{d_0}{\lambda}} \cdot \left|E\left(d'\right)\right|^2, \\ r_{d''}(t) &= \frac{\sqrt{G_{T,d''} G_{R,d''}}}{d_0} e^{-j2\pi\frac{d_0}{\lambda}} \cdot \left|E_r\left(d''\right)\right|^2, \end{aligned} \tag{6}$$

where $G_{T,d'}$ and $G_{R,d'}$ are the antenna field radiation patterns of the Tx-UAV and Rx-UAV antennas in LOS direction, respectively, and $G_{T,d''}$ and $G_{R,d''}$ are the antenna field radiation patterns of the Tx-UAV and Rx-UAV antennas along the direction of the ground reflection path, respectively.

$h_{\text{Tx-UAV}}$ and $h_{\text{Rx-UAV}}$ are the heights of the Tx-UAV and Rx-UAV, respectively. The propagation distance and the phase difference by difference of the LOS path and the ground reflection path are denoted by

$$\begin{aligned} \Delta d &= \frac{2h_{\text{Tx-UAV}} h_{\text{Rx-UAV}}}{d_c}, \\ \Delta\theta &= \frac{4\pi h_{\text{Tx-UAV}} h_{\text{Rx-UAV}}}{\lambda d_c}. \end{aligned} \tag{7}$$

The received signal power can be approximately calculated as follows:

$$\begin{aligned} P_{\text{Rx-UAV}}(d_c) &\approx P_{\text{Tx-UAV}}\left(\frac{\lambda}{4\pi}\right)^2 \frac{G_T G_R}{d_c^2}\left(\frac{4\pi h_{\text{Tx-UAV}} h_{\text{Rx-UAV}}}{\lambda d_c}\right)^2 \\ &= P_{\text{Tx-UAV}} G_T G_R h_{\text{Tx-UAV}}^2 h_{\text{Rx-UAV}}^2 d_c^{-4}, \end{aligned} \tag{8}$$

where G_T denotes the approximate value for $G_{T,d'}$ and $G_{T,d''}$. G_R is the approximate value for $G_{R,d'}$ and $G_{R,d''}$, respectively.

The path loss expression of the A2AT-R model is given by

$$PL_{\text{A2AT-R}}(\text{dB}) \approx 10\log_{10}\left[\frac{1}{4G_T G_R}\left(\frac{4\pi d_c}{\lambda}\right)^2 \cdot \left(\frac{2\pi h_{\text{Tx-UAV}} h_{\text{Rx-UAV}}}{\lambda d_c}\right)\right]. \tag{9}$$

2.2. The Modified Log-Distance Model. The modified Log-Distance model for the channel modeling of UAV

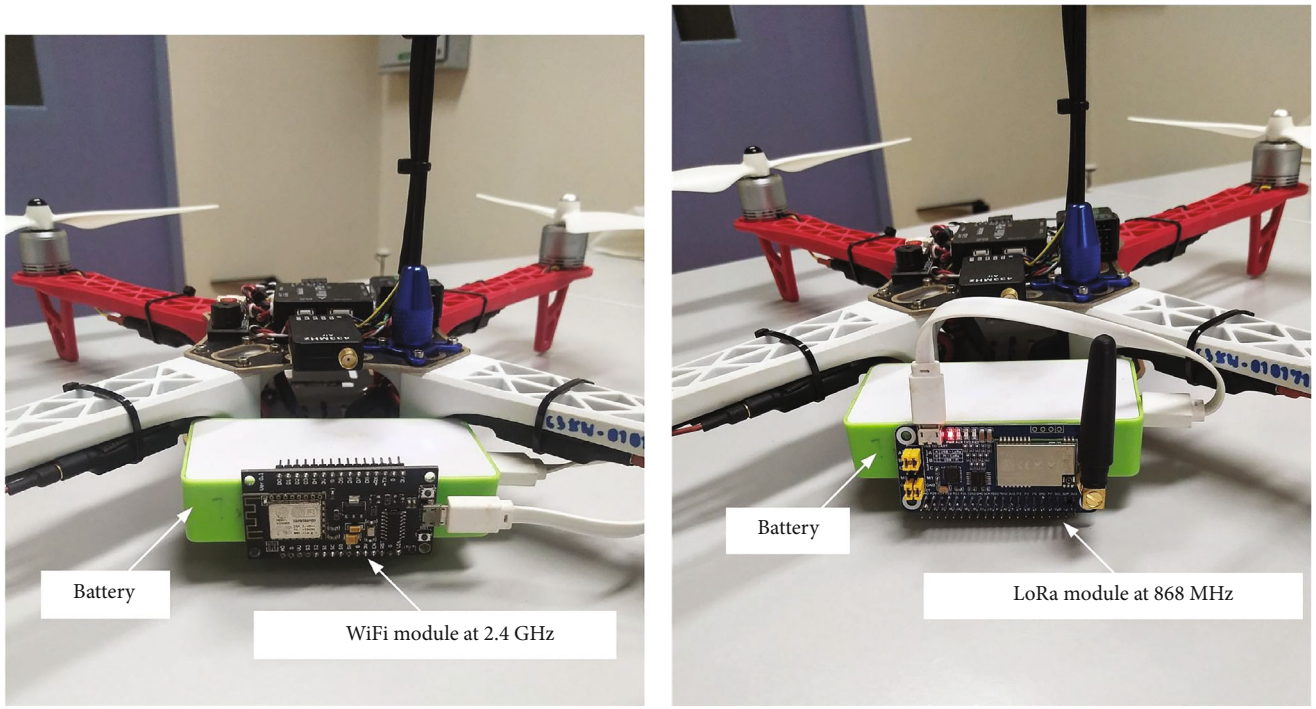

(a) UAV-enabled WiFi module (b) UAV-enabled LoRa module

Figure 2: Illustration of UAV-enabled wireless communication modules.

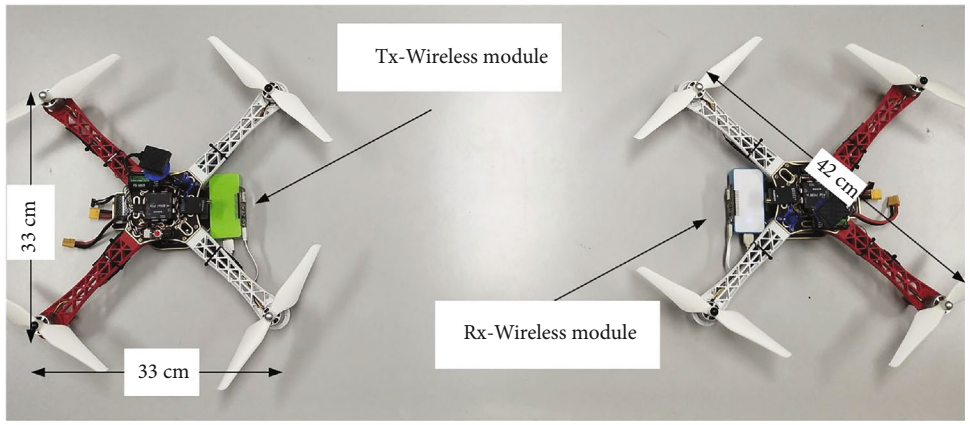

Figure 3: Top view of the Tx-UAV and Rx-UAV [36].

communications can be extended from the conventional Log-Distance model [35] as

$$PL_f = K\left(\frac{d_c}{d_0}\right)^{\alpha}, \tag{10}$$

where K denotes the unit-less scaling factor and α is the path loss exponent. Then, the path loss in dB scale is given by

$$PL_f(\text{dB}) = K(\text{dB}) + 10\alpha \log_{10}\left(\frac{d_c}{d_0}\right). \tag{11}$$

For the modified Log-Distance model, one form closely similar to the general form of the Log-Distance model is the floating intercept model given by

$$PL_f(\text{dB}) = 10\alpha(h_{\text{Rx-UAV}}) \log_{10} d_c + \beta(h_{\text{Rx-UAV}}), \tag{12}$$

where α and β are usually jointly determined by minimizing the mean square error between the model and the empirical measurements. The $h_{\text{Rx-UAV}}$ denotes the height

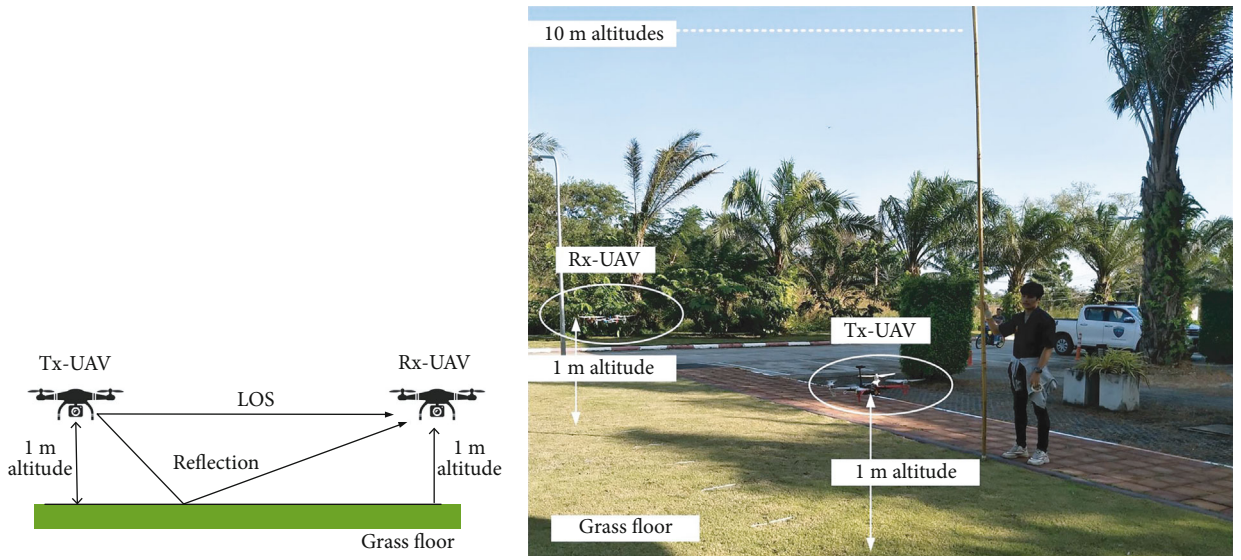

Figure 4: Test of path loss characteristics in CM1: the A2A ground reflection model from the grass floor (left) and the measurement setup scenario (right) [36].

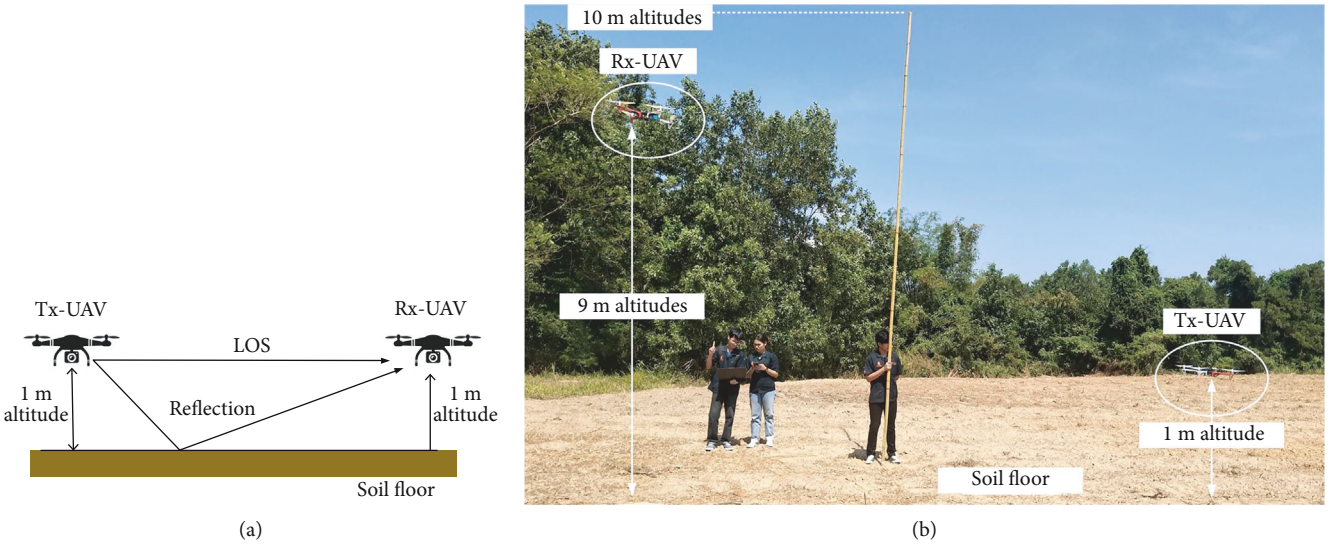

Figure 5: Test of path loss characteristics in CM2: the A2A ground reflection model from the soil floor (left) and the measurement setup scenario (right) [36].

of Rx-UAV, and $\alpha(h_{\text{Rx-UAV}})$ and $\beta(h_{\text{Rx-UAV}})$ determined based on measurement are given by

$$\begin{aligned}\alpha(h_{\text{Rx-UAV}}) &= \max\left(3.9 - 0.9\log_{10}(h_{\text{Rx-UAV}}), 2\right),\\ \beta(h_{\text{Rx-UAV}}) &= -8.5 + 20.5\log_{10}(\min\left(h_{\text{Rx-UAV}}, h_{\text{FSPL}}\right)),\end{aligned} \tag{13}$$

where h_{FSPL} is the height where free-space propagation loss (FSPL).

Finally, the modified Log-Distance model which the antenna characteristics, certain propagation environment, and frequency term are considered. The expression is given by

$$\begin{aligned}PL(\text{dB}) = PL_f(\text{dB}) &+ 10\alpha(h_{\text{Rx-UAV}})\log_{10}\left(\frac{d_c}{d_0}\right)\\ &- 10\log_{10}\left(\frac{h_{\min}}{\Delta h}\right) + C_l + 10\log_{10}(1 + f_c),\end{aligned} \tag{14}$$

where $\Delta h = |h_{\text{Rx-UAV}} - h_{\min}|$, $h_{\min}$ is the minimum height of the Rx-UAV that gives the lowest path loss for a given environment, and C_l is a constant polarization loss from UAV antenna orientations.

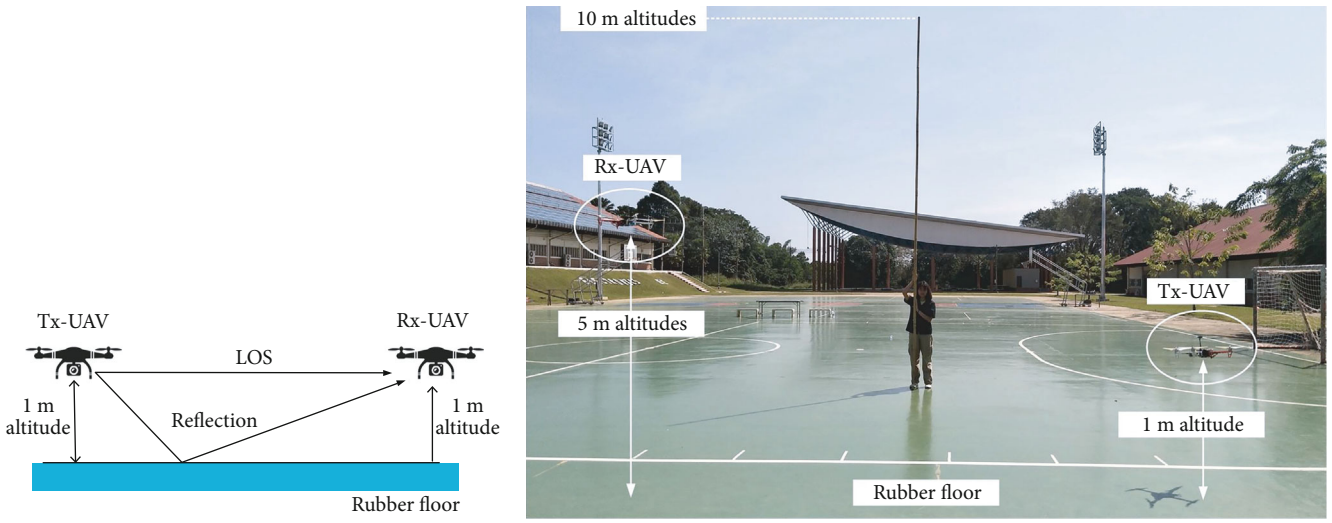

Figure 6: Test of path loss characteristics in CM3: the A2A ground reflection model from the rubber floor (left) and the measurement setup scenario (right) [36].

3. Measurement Setup

This section describes the measurement setup in different scenarios for the proposed ground reflection model. The quadcopter drone as a Tx-UAV and Rx-UAV is used to analyze the channel characterization in UAV-enabled wireless communication. The UAV-enabled wireless modules where the WiFi module is set up by using EPS8266 microcontroller at 2.4 GHz as shown in Figure 2(a), while the LoRa module at 868 MHz is shown in Figure 2(b). Both the wireless modules are supplied by using the battery 1,800 mAh of the power consumption. The weight of the UAV was 0.5 kg and the flight time is limited to 15 min. Figure 3 illustrates the top view of Tx-UAV and Rx-UAV where the dimension of UAV was 42 cm in length of UAV frame, and the propeller is the 10-inch length.

In the experiment, the height of Tx-UAV $h_{\text{Tx-UAV}}$ at 1 m altitude is fixed, and the height of Rx-UAV $h_{\text{Rx-UAV}}$ from 1 m to 10 m altitudes is varied. The separation distance d_c between Tx-UAV and Rx-UAV is 10 m. Figure 4 shows the experiment of path loss characteristic in CM1 grass floor where the A2A ground reflection model from the grass floor (left) and the measurement setup scenario (right). Likewise, the measurement setup in CM2 soil floor and CM3 rubber floor is shown in Figure 5 and Figure 6, respectively. To evaluate the path loss characteristics, we collected the RSSI data from the Rx-UAV via an application program interface (API) by using a blink application for the WiFi module. Besides, the LoRa NodeJS software application is used for the LoRa module. For the LoRa module setup, the Tx-UAV side is set as a LoRa gateway and set as a LoRa endpoint for the Rx-UAV. The measurement setup parameters are listed in Table 1.

Table 1: Measurement setup parameters.

Parameters	Values
Carrier frequency	2.4 GHz, 868 MHz
Power transmit (WiFi module)	20 dBm
Power transmit (LoRa module)	20 dBm
Tx-UAV height	1 m
Rx-UAV height	1-10 m
Flight time	15 min
Separation distance	10 m
Antenna gain (WiFi module)	2.1 dBi
Antenna gain (LoRa module)	3.5 dBi
Data rate (WiFi module)	1 Mbps
Data rate (LoRa module)	37.4 kbps

4. Results and Discussion

In this section, the results of measurement data from the different CM scenario cases, the analytical A2AT-R model, and the modified Log-Distance model are described. For the experiment of the WiFi module at 2.4 GHz frequency, the path loss characteristics are shown in Figure 7. Figure 7(a) shows the path loss versus the Rx-UAV altitudes in the CM1 grass floor. It can be seen that the analytical A2AT-R path loss model is from 89.31 dB to 99.35 dB. On the other hand, the modified Log-Distance path loss model ranges from 76.23 dB to 87.74 dB where the constant polarization loss C_l was 1.5 dB. It can be observed that the path loss of the analytical A2AT-R model is higher than the modified Log-Distance model to 11.61 dB. Nevertheless, the path loss of measurement data in this scenario case ranges from 78.32 dB to 90.12 dB which is related to the modified Log-Distance model along with the increasing of Rx-UAV altitudes.

Figure 7(b) shows the path loss characteristics in the CM2 soil floor scenario. The measurement data is from 77.45 dB to 91.21 dB along with the increase of Rx-UAV altitudes. It can be seen that the measurement data of path loss

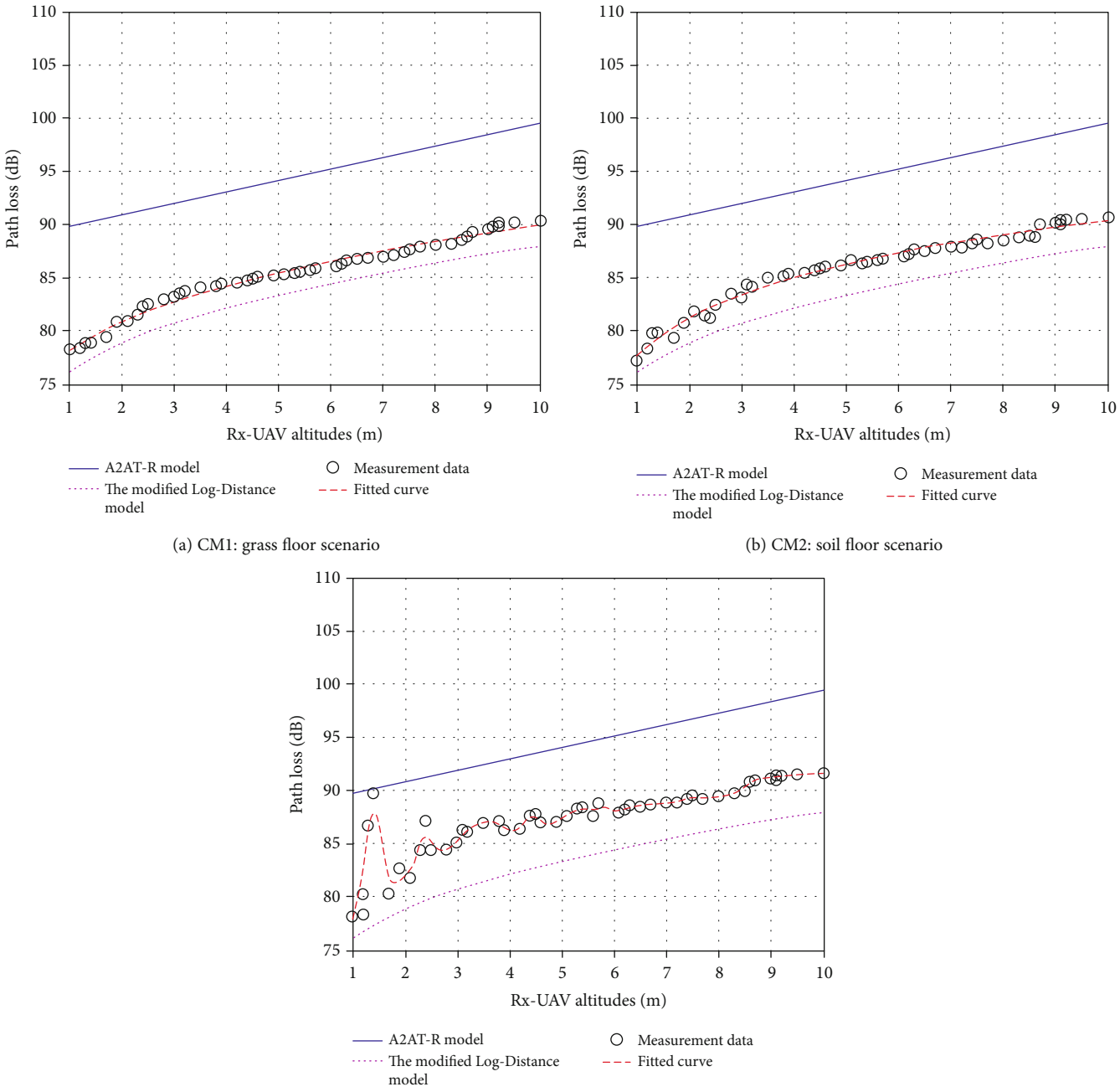

(a) CM1: grass floor scenario

(b) CM2: soil floor scenario

(c) CM3: rubber floor scenario

Figure 7: Path loss characteristics of A2A channel modeling by using WiFi module at 2.4 GHz.

depend on the modified Log-Distance model. Meanwhile, we observe that the path loss characteristics in the CM3 rubber floor scenario case are shown in Figure 7(c). The propagation affected from the ground reflection is encountered at 1 m to 3 m. With the result of this situation, the path loss level has closely fluctuated to the analytical A2AT-R model. When the Rx-UAV over at 3 m altitudes, it can observe that the path loss characterized is still be correlated with the modified Log-Distance model.

For the experiment of the LoRa module at 868 MHz frequency, the path loss characteristics are shown in Figure 8. Figure 8(a) shows the path loss versus the Rx-UAV altitudes in the CM1 grass floor. As a result, the analytical A2AT-R path loss model ranges from 85.01 dB to 94.65 dB; additionally, the modified Log-Distance path loss model ranges from 70.04 dB to 83.66 dB. Comparing the path loss values, the LoRa module at 868 MHz is smaller than the WiFi module at 2.4 GHz approximately as 4.30 dB for the A2AT-R model and 6.19 dB for the modified Log-Distance model. The measurement data in Figure 8(a) is still be correlated with the modified Log-Distance model. The path loss of measurement data ranges from 75.04 dB to 86.23 dB for this scenario case.

Figure 8(b) shows the path loss characteristics in the CM2 soil floor scenario case. The path loss of measurement

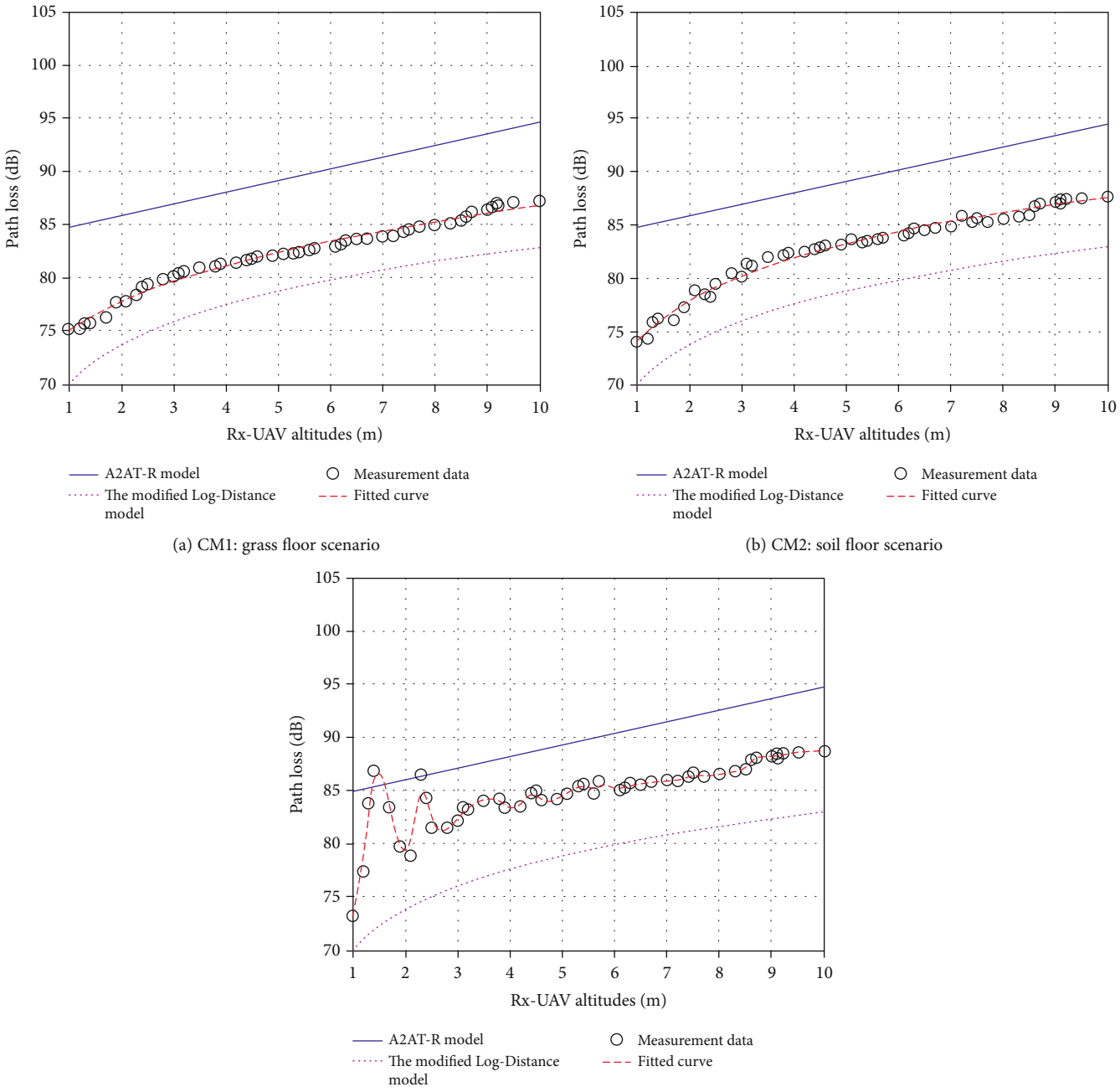

(a) CM1: grass floor scenario

(b) CM2: soil floor scenario

(c) CM3: rubber floor scenario

Figure 8: Path loss characteristics of A2A channel modeling by using LoRa module at 868 MHz.

data is varied from 74.24 dB to 87.43 dB, and then, the propagation effect of the ground reflection is uncorrelated. In this scenario case, the path loss measurement data is dependent on the modified Log-Distance model along with the increasing of the Rx-UAV altitudes. Likewise, the path loss measurement data in the CM3 rubber floor scenario case is shown in Figure 8(c) which is affected by the ground reflection. At the Rx-UAV 1 m to 3 m altitudes, the data closely fluctuates to the analytical A2AT-R path loss model. In this scenario, the path loss measurement data are correlated to the modified Log-Distance model after the Rx-UAV is higher than 3 m altitudes.

To discuss the measurement scenario cases, it can be seen that the propagation affected from the ground reflection is encountered in the CM3 rubber floor scenario, in particular, when the Rx-UAV hovered at 1 m to 3 m. The path loss characteristics are closely related to the analytical A2AT-R model. Besides, it can be observed that the path loss measurement data over the Rx-UAV 3 m altitudes was correlated with the modified Log-Distance model along with the separation distance between Tx-UAV and Rx-UAV. Moreover, it clear that there is no ground reflection effect from the CM1 grass floor and CM2 soil floor.

5. Conclusions

In this paper, we presented the empirical path loss channel characterization of A2A ground reflection channel modeling for small UAVs-enabled wireless communications. Under the condition of different ground reflection scenarios, the path loss characteristics from WiFi-based 2.4 GHz and LoRa-based 868 MHz wireless communication modules have been investigated by using simulation and experimental data. Moreover, the simulation of the A2AT-R model and the modified Log-Distance model where CM1 grass floor, CM2 soil floor, and CM3 rubber floor have studied the condition of different ground reflection scenarios. It can be shown that the impact of ground reflection is encountered in CM3 from the rubber floor; in the same way, there is no ground reflection effect from the grass floor and soil floor, by using WiFi and LoRa modules. To summarize the study of this work, the analytical A2AT-R model can simulate path loss characteristics based on the separation distance of UAVs, the height of UAVs, the antenna gains of UAVs, and the impact of ground reflection. While the modified Log-Distance model can provide the path loss characteristic based on the dependency of free space loss, the separation distance of UAVs, the height of UAVs, the polarization loss, and the empirical measurement for A2A-CM. In future work, the path loss characteristic will be investigated by using the modified Log-Distance model in the long-range communication at least 1 km of the separation distance between Tx-UAV and Rx-UAV for A2A-CM with LoRa 868 MHz module.

Data Availability

The data that support the findings of this study are available from the corresponding author upon reasonable request.

Conflicts of Interest

The authors declare that there are no conflicts of interest concerning the publication of this paper.

Acknowledgments

This work was financially supported by a KMITL research fund in the Academic Melting Pot scholarship project.

References

[1] S. Sruthy and S. N. George, "WiFi enabled home security surveillance system using Raspberry PI and IoT module," in *Proceeding of IEEE International Conference on Signal Processing, Informatics, Communication and Energy Systems (SPICES)*, pp. 1–6, Kollam, India, 2017.

[2] M. L. Liya and M. Aswathy, "LoRa technology for Internet of Things (IoT): a brief survey," in *Proceeding of Fourth International Conference on I-SMAC*, pp. 8–13, Palladam, India, 2020.

[3] M. Kanj, V. Savaux, and M. le Guen, "A tutorial on NB-IoT physical layer design," *IEEE Communications Surveys & Tutorials*, vol. 22, no. 4, pp. 2408–2446, 2020.

[4] A. Lavric, A. I. Petrariu, and V. Popa, "Sig Fox communication protocol: the new Era of IoT," in *Proceeding of International Conference on Sensing and Instrumentation in IoT Era (ISSI)*, pp. 1–4, Lisbon, Portugal, 2019.

[5] M. Haghi, S. Neubert, A. Geissler et al., "A flexible and pervasive IoT-based healthcare platform for physiological and environmental parameters monitoring," *IEEE Internet of Things Journal*, vol. 7, no. 6, pp. 5628–5647, 2020.

[6] F. Zhu, Y. Lv, Y. Chen, X. Wang, G. Xiong, and F.-Y. Wang, "Parallel transportation systems: toward IoT-enabled smart urban traffic control and management," *IEEE Transactions on Intelligent Transportation Systems*, vol. 21, no. 10, pp. 4063–4071, 2020.

[7] M. S. Farooq, S. Riaz, A. Abid, K. Abid, and M. A. Naeem, "A survey on the role of IoT in agriculture for the implementation of smart farming," *IEEE Access*, vol. 7, pp. 156237–156271, 2019.

[8] F. Cirillo, D. Gomez, L. Diez, I. Elicegui Maestro, T. B. J. Gilbert, and R. Akhavan, "Smart city IoT services creation through large-scale collaboration," *IEEE Internet of Things Journal*, vol. 7, no. 6, pp. 5267–5275, 2020.

[9] M. Ballerini, T. Polonelli, D. Brunelli, M. Magno, and L. Benini, "NB-IoT versus LoRaWAN: an experimental evaluation for industrial applications," *IEEE Transactions on Industrial Informatics*, vol. 16, no. 12, pp. 7802–7811, 2020.

[10] W. Khawaja, I. Guvenc, D. W. Matolak, U.-C. Fiebig, and N. Schneckenburger, "A survey of air-to-ground propagation channel modeling for unmanned aerial vehicles," *IEEE Communications Surveys & Tutorials*, vol. 21, no. 3, pp. 2361–2391, 2019.

[11] F. Ono, T. Kagawa, H. Tsuji, R. Miura, and F. Kojima, "Measurements on C-band air-to-air channel for coexistence among multiple unmanned aircraft systems," in *Proceeding of International Conference on Unmanned Aircraft Systems*, pp. 1160–1164, Miami, FL, USA, June 2017.

[12] Z. Xiao, P. Xia, and X. G. Xia, "Enabling UAV cellular with millimeter-wave communication: potentials and approaches," *IEEE Communications Magazine*, vol. 54, no. 5, pp. 66–73, 2016.

[13] S. Duangsuwan, C. Teekapakvisit, and M. M. Maw, "Development of soil moisture monitoring by using IoT and UAV-SC for smart farming application," *Advances in Science, Technology and Engineering Systems Journal*, vol. 5, no. 4, pp. 381–387, 2020.

[14] C. D. Lopez and L. F. Giraldo, "Optimization of energy and water consumption on crop irrigation using UAVs via path design," in *Proceeding of IEEE Colombian Conference on Automatic Control (CCAC)*, pp. 1–5, Medellin, Colombia, Oct. 2019.

[15] M. R. Seye, B. Ngom, B. Gueye, and M. Diallo, "A study of LoRa coverage: range evaluation and channel attenuation model," in *Proceeding of International Conference on Smart Cities and Communities (SCCIC)*, pp. 1–4, Ouagadougou, Burkina Faso, July 2018.

[16] J. Xiang, X. Zhu, T. Zhou, and Y. Su, "A low power and ultra-long range UAV attitude measurement system," in *Proceeding of IEEE 4th Information Technology and Mechatronics Engineering Conference (ITOEC)*, pp. 275–278, Chongqing, China, December 2018.

[17] Z. Yuan, J. Jin, L. Sun, K.-W. Chin, and G.-M. Muntean, "Ultra-reliable IoT communications with UAVs: a swarm use case," *IEEE Communications Magazine*, vol. 56, no. 12, pp. 90–96, 2018.

[18] J. Oh, D.-W. Lim, and K.-M. Kang, "Unmanned aerial vehicle identification success probability with LoRa communication approach," in *Proceeding of IEEE 31st Annual International Symposium on Personal, Indoor and Mobile Radio Communications*, pp. 1–6, London, UK, August–September 2020.

[19] G. Baruffa, L. Rugini, V. Mecarelli, L. Germani, and F. Frescura, "Coded LoRa performance in wireless channels," in *Proceeding of IEEE 30st Annual International Symposium on Personal, Indoor and Mobile Radio Communications*, pp. 1–6, Istanbul, Turkey, September 2019.

[20] P. Jorke, S. Bocker, F. Liedmann, and C. Wietfeld, "Urban channel models for smart city IoT-networks based on empirical measurements of LoRa-links at 433 and 868 MHz," in *Proceeding of IEEE 28st Annual International Symposium on Personal, Indoor and Mobile Radio Communications*, pp. 1–6, Montreal, QC, Canada, October 2017.

[21] L.-Y. Chen, H.-S. Huang, C.-J. Wu, Y.-T. Tsai, and Y.-S. Chang, "A LoRa-based air quality monitor on unmanned aerial vehicle for smart city," in *Proceeding of International Conference on System Science and Engineering (ICSSE)*, pp. 1–5, New Taipei, Taiwan, June 2018.

[22] M. F. Lima Pereira, P. E. Cruvinel, G. M. Alves, and J. M. G. Beraldo, "Parallel computational structure and semantics for soil quality analysis based on LoRa and apache spark," in *Proceeding of IEEE 14th International Conference on Semantic Computing (ICSC)*, pp. 332–336, San Diego, CA, USA, February 2020.

[23] Y. Zhang, J. Wen, G. Yang, Z. He, and X. Luo, "Air-to-air path loss prediction based on machine learning methods in urban environments," *Wireless Communications and Mobile Computing*, vol. 2018, 10 pages, 2018.

[24] S. Duangsuwan and M. M. Maw, "Comparison of path loss prediction models for UAV and IoT air-to-ground communication system in rural precision farming environment," *Journal of Communications*, vol. 16, no. 2, pp. 60–66, 2021.

[25] O. Ahmadien, H. F. Ates, T. Baykas, and B. K. Gunturk, "Predicting path loss distribution of an area from satellite Images using deep learning," *IEEE Access*, vol. 8, pp. 64982–64991, 2020.

[26] S. K. Goudos, G. V. Tsoulos, G. Athanasiadou, M. C. Batistatos, K. E. Psannis, and D. Zarbouti, "Artificial neuron network optimal modeling and optimization of UAV measurements for mobile communications using the L-SHADE algorithm," *IEEE Transaction on Antennas and Propagation*, vol. 67, no. 6, pp. 4022–4031, 2019.

[27] C. Yan, L. Fu, J. Zhang, and J. Wang, "A comprehensive survey on UAV communication channel modeling," *IEEE Access*, vol. 7, pp. 107769–107792, 2019.

[28] M. A. Bellido-Manganell, "Design approach of a future air-to-air data link," in *Proceeding of IEEE/AIAA 37th Digital Avionics Systems Conference (DASC)*, pp. 1–9, London, UK, September 2018.

[29] L. Zhou, Z. Yang, G. Zhao, S. Zhou, and C.-X. Wang, "Propagation characteristics of air-to-air channels in urban environments," in *Proceeding of IEEE Global Communications Conference (GLOBECOM)*, pp. 1–6, Abu Dhabi, United Arab Emirates, December 2018.

[30] U. C. Çabuk, M. Tosun, R. H. Jacobsen, and O. Dagdeviren, "Path loss estimation of air-to-air channels for FANETs over Rugged Terrains," in *Proceeding of 28th Signal Processing and Communications Applications Conference (SIU)*, pp. 1–4, Gaziantep, Turkey, October 2020.

[31] D. Becker, U.-C. Fiebig, and L. Schalk, "Wideband channel measurements and first findings for low altitude drone-to-drone links in an urban scenario," in *Proceeding of 14th European Conference on Antennas and Propagation (EuCAP)*, pp. 1–5, Copenhagen, Denmark, March 2020.

[32] Z. Wei and J. Geng, "Time-variant PDFs of AODs and AOAs for ground scattering in low-altitude air-to-air communication over open area," *IEEE Communications Letters*, vol. 25, no. 3, pp. 1–5, 2021.

[33] M. Walter, D. Shutin, D. W. Matolak, N. Schneckenburger, T. Wiedemann, and A. Dammann, "Analysis of non-stationary 3D air-to-air channels using the theory of algebraic curves," *IEEE Transactions on Wireless Communications*, vol. 18, no. 8, pp. 3767–3780, 2019.

[34] X. Zhang, J. Liu, F. Gu, D. Ma, and J. Wei, "An extended 3-D ellipsoid model for characterization of UAV air-to-air channel," in *Proceeding of IEEE International Conference on Communications (ICC)*, pp. 1–6, Shanghai, China, May 2019.

[35] R. Amorim, H. Nguyen, P. Mogensen, I. Z. Kovacs, J. Wigard, and T. B. Sorensen, "Radio channel modeling for UAV communication over cellular networks," *IEEE Wireless Communications Letters*, vol. 6, no. 4, pp. 514–517, 2017.

[36] S. Duangsuwan, "Measurement of path loss characterization and prediction modeling for swarm UAVs air-to-air wireless communication systems," *Journal of Communications*, vol. 16, no. 6, pp. 228–235, 2021.